

1 **FOSL2 Directly Regulates FSHR and CYP11A1 Transcription: An Essential**
2 **Transcription Factor for Gonadotropin-Dependent Folliculogenesis**

3 Hongru Shi^{1†}, Chaoli Chen^{2†}, Zaohong Ran^{1†}, Jianning Liao¹, Zian Wu¹, Xiaodong
4 Wang¹, Yongheng Zhao¹, Wenkai Ke¹, Bowen Tan¹, Yun Liu¹, Wei Ren^{2*}, Xiang Li^{1*},
5 Changjiu He^{1*}

6 ¹ Key Laboratory of Agricultural Animal Genetics, Breeding and Reproduction of
7 Ministry of Education, College of Animal Sciences and Technology, Huazhong
8 Agricultural University, Wuhan 430070, PR China;

9 ² Department of Obstetrics, Maternal and Child Health Hospital of Hubei Province,
10 Wuhan 430070, PR China;

11 [†]These authors contributed equally to this work.

12 ***Corresponding Author:**

13 Wei Ren, Orcid ID: 0000-0002-1061-276X;

14 Email: 1393600775@qq.com; Maternal and Child Health Hospital of Hubei Province,
15 Wuhan 430070, China.

16 Xiang Li, Orcid ID: 0000-0002-9168-1598;

17 Email: xxianglli@mail.hzau.edu.cn; Huazhong Agricultural University, Wuhan
18 430070, China.

19 Changjiu He, Orcid ID: 0000-0002-0350-9799;

20 Email: chungjoe@mail.hzau.edu.cn; Huazhong Agricultural University, Wuhan
21 430070, China.

22

23 **Short title:** Fosl2 functions on GTH-dependent folliculogenesis

24

25 **ABSTRACT**

26 Fosl2, a member of the AP-1 family, has been widely studied in the fields of
27 tumorigenesis and immune response, but its role in folliculogenesis remains unclear.
28 In this investigation, we presented comprehensive in vitro and in vivo evidence to
29 precisely define the biological functions of Fosl2 in folliculogenesis. Fosl2 in both
30 mouse and sheep, we demonstrated that the knockdown of *Fosl2* effectively inhibited
31 cell proliferation and promoted cell apoptosis in both primary GCs and the GCs of
32 cultured gonadotropin (GTH)-dependent follicles. To explore the in-vivo function of
33 Fosl2, we generated an ovarian GC-specific conditional knockout (CKO) mouse
34 model. CKO mice showed impaired GTH-dependent folliculogenesis, leading to
35 disrupted estrous cycles and infertility in female mice. Subsequent bioinformatics
36 analysis and experimental results indicated that Fosl2 regulates the transcription of
37 FSHR and CYP11A1. These findings unveiled the essential role of Fosl2 in governing
38 the development of GTH-dependent folliculogenesis, thereby providing a novel
39 strategy for elucidating GTH-dependent folliculogenesis mechanisms and treating
40 ovarian dysfunction.

41 **Keywords:** Fosl2, folliculogenesis, granulosa cell, estradiol, gonadotropin-dependent
42 follicle

43

44 INTRODUCTION

45 Infertility has emerged as a significant global health concern, with impaired
46 folliculogenesis representing a critical factor in female reproductive dysfunction[1].
47 Ovarian follicles, the fundamental functional units of ovary comprising oocytes and
48 granulosa cells (GCs), serve as pivotal determinants of female fertility. GCs orchestrate
49 folliculogenesis through multifaceted roles in oocyte-granulosa cell communication,
50 metabolic regulation, hormonal synthesis, and signal transduction [2-6]. The granulosa
51 cells are indispensable for oocyte maturation, GTH-dependent folliculogenesis (antrum
52 formation and expansion), and post-ovulatory luteinization [7-9]. The GTH-dependent
53 stage constitutes a decisive period governed by integrated endocrine networks
54 involving gonadotropins, steroid hormones, growth factors, and inhibins, which
55 collectively dictate follicular fate determination [10-13]. Elucidating regulatory
56 mechanisms during this critical developmental period remains essential for advancing
57 reproductive research.

58 Previous studies have reported numerous transcription factors that play key roles
59 in the ovaries [14-16]. Fos-like antigen 2 (*Fosl2*), a component of the transcription factor
60 AP-1 family [17], modulates cellular processes including growth regulation, and
61 immune responses [18-26]. It has been reported that homozygous mice with systemic
62 knockout of *Fosl2* died within one week after birth [27], and studies have also shown
63 that abnormal expression of *Fosl2* can cause some diseases, such as asthma and
64 pulmonary fibrosis[28, 29], suggesting that *Fosl2* may play an important role in the
65 regulation of animal organism. Although Fos family members regulate ovulation-
66 related genes[30], and bioinformatic analyses implicate *Fosl2* in polycystic ovary
67 syndrome [31]. The specific reproductive functions of *Fosl2* in folliculogenesis remain
68 unknown.

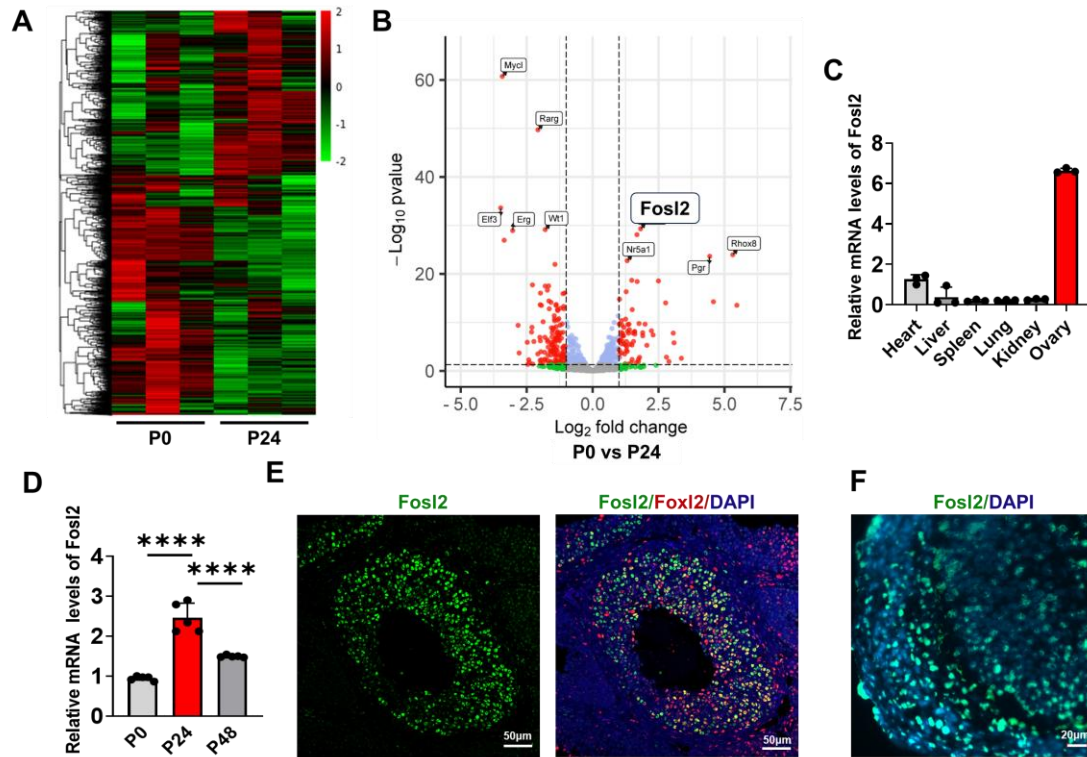
69 This study demonstrates that *Fosl2* deficiency disrupts GTH-dependent
70 folliculogenesis and induces female infertility. Transcriptome analysis revealed *Fosl2*
71 is highly expressed in ovarian granulosa cells and is induced by gonadotropin. GC-
72 specific knockdown and conditional knockout impaired granulosa cell proliferation,

73 suppressed GTH-dependent folliculogenesis, and disrupted estrous cycle.
74 Mechanistically, *Fosl2* directly regulates the transcription of *FSHR* and *CYP11A1* to
75 exert its function. Our findings establish *Fosl2* as an essential transcription factor of
76 GTH-dependent folliculogenesis, providing new insights for improving the
77 reproductive performance of humans and animals.

78 **RESULTS**

79 **1. Characterization of the *Fosl2***

80 In order to further explore the transcription factors that play an important role in
81 the development of follicles, we performed transcriptome analysis in mice ovarian
82 granulosa cells from PMSG 0h to PMSG 24h [32]. The expression of the transcription
83 factor *Fosl2* was found to be significantly induced by PMSG (Figure 1A, B). The tissue
84 expression profile of *Fosl2* in mice was mapped by qRT-PCR, confirming that *Fosl2*
85 was highly expressed in the ovary (Figure 1C). The results of qRT-PCR further
86 confirmed that *Fosl2* expression was significantly induced by PMSG (Figure 1D.).
87 Immunofluorescence staining confirmed that *Fosl2* was mainly localized in GCs of
88 ovarian follicles both in mouse and sheep (Figure 1E, F). These findings suggest that
89 *Fosl2* is mainly localized in ovarian GCs and induced by PMSG.



90

91 **Figure 1. Fosl2 is highly expressed in ovarian GCs and induced by PMSG (A)**
 92 Heatmap of the up-regulated genes in mGCs after PMSG injection. (B) Transcriptome
 93 analysis was used to identify the up-regulated and down-regulated genes of
 94 transcription factor in ovarian GCs after PMSG injection. Three GCs samples derived
 95 from six mice per group were used for RNA-seq. (C) Tissue expression profile of *Fosl2*
 96 gene in mice, n=3. (D) Expression of *Fosl2* gene in mouse ovarian GCs 0, 24, 48 hours
 97 after PMSG injection, n=5. (E) Immunofluorescence staining showed the localization
 98 of Fosl2 protein in follicles of mouse. Green is a positive stain for Fosl2 protein.
 99 Nuclear staining was performed with DAPI. (F) Immunofluorescence staining showed
 100 the localization of Fosl2 protein in follicles of sheep. Green is a positive stain for Fosl2
 101 protein. Nuclear staining was performed with DAPI. Statistical significance were
 102 determined using one-way ANOVA followed by Tukey's post hoc test, values were
 103 mean \pm SD. Significant differences were denoted by **P<0.01, ***P<0.005. The
 104 experiments were repeated independently two times, yielding consistent results.

105

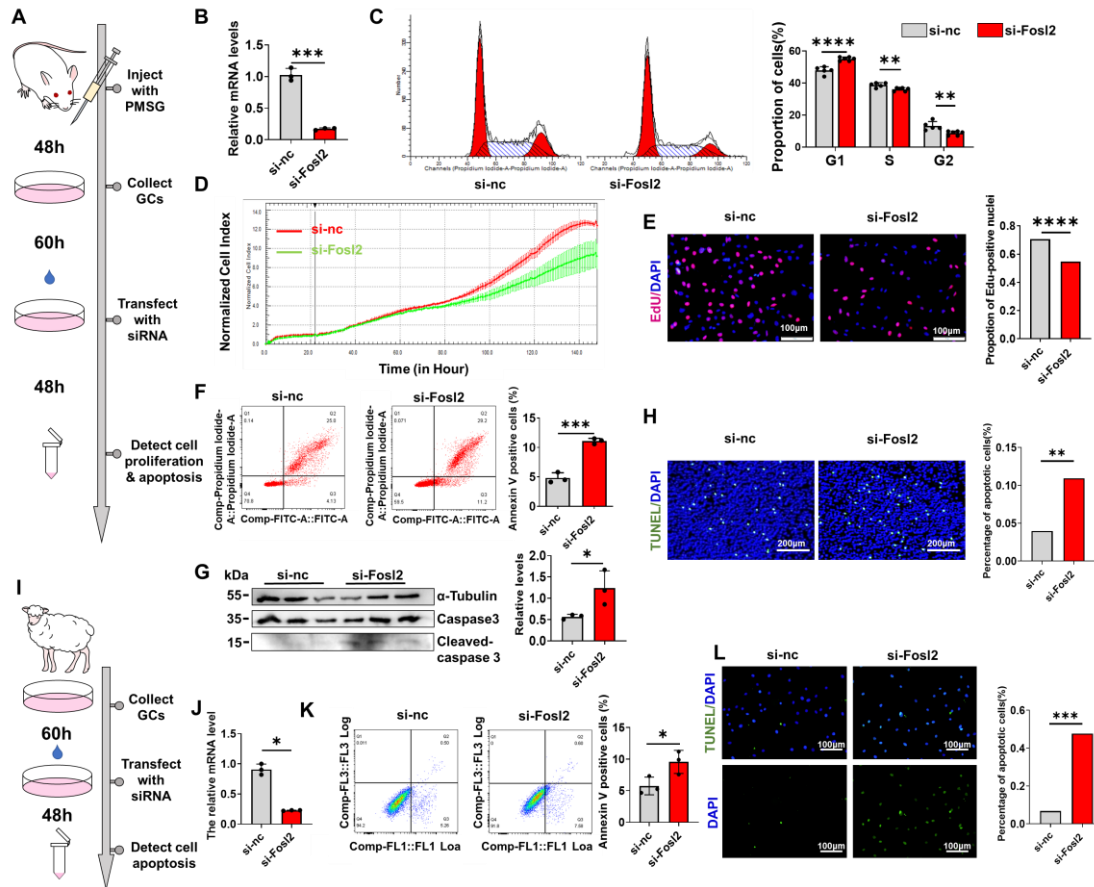
106 **2. Knockdown of *Fosl2* inhibits proliferation and promotes apoptosis in GCs**

107 To investigate the function of *Fosl2* in ovarian GCs, mouse primary GCs were
108 isolated and transfected with siRNA targeting *Fosl2*, with knockdown efficiency
109 confirmed (Figure 2A, B). Flow cytometric analysis of cell cycle distribution revealed
110 that *Fosl2*-knockdown significantly increased the proportion of cells in G1 phase while
111 reducing populations in S and G2 phases (Figure 2C), indicating G1 phase arrest and
112 impaired DNA synthesis. Real-time cell analysis (RTCA) showed delayed entry into
113 the rapid proliferation phase and reduced cell index peak in *Fosl2*-knockdown GCs
114 (Figure 2D). EdU staining further demonstrated suppressed proliferation in *Fosl2*-
115 knockdown cells (Figure 2E).

116 Then the apoptosis of *Fosl2*-knockdown GCs was detected. Flow cytometry
117 analysis showed that knockdown of *Fosl2* resulted in a significant increase in the
118 proportion of annexin-V-positive cells, indicating an increase in GCs at an early
119 apoptotic stage (Figure 2F). Knockdown of *Fosl2* significantly increased the expression
120 of the apoptosis marker protein Cleaved-Caspase3 (Figure 2G). Further TUNEL
121 staining showed that the proportion of apoptotic cells was significantly increased
122 (Figure 2H). Sheep primary GCs were isolated and transfected with siRNA targeting
123 *Fosl2* (Figure 2I, J). Similarly, apoptosis of cells is enhanced (Figure 2K, L).
124 Conversely, *Fosl2* overexpression (Figure S1A) reduced the proportion of early
125 apoptotic cells (Figure S1B), confirming the regulatory role of *Fosl2* in apoptosis.

126 These results demonstrate that *Fosl2* knockdown inhibits proliferation and
127 promotes apoptosis in ovarian GCs.

128



129

130 **Figure 2. *Fosl2* knockdown on GCs inhibits cell proliferation and promotes**

131 **apoptosis.** (A-I) Knockdown *Fosl2* in GCs of mouse. (A) Schematic representation of

132 the knockdown or overexpress of *Fosl2* in primary mouse GCs. (B) Efficiency analysis

133 of *Fosl2* interference using qRT-PCR, n=3. The scrambled siRNA was used as *si-nc* in

134 this study. (C) Effect of *Fosl2*-knockdown on cell cycle, left: Representative images of

135 cell cycle by flow cytometry, right: Cell cycle distribution, n=5(*si-nc*), 6(*si-Fosl2*). (D)

136 Effect of *Fosl2*-knockdown on rapid cell proliferation. (E) EdU staining of *Fosl2*-

137 knockdown cells, with red dots representing newly divided cells, left: Representative

138 fluorescence images of EdU staining, right: Cell proliferation rate. (F) Flow cytometry

139 results of apoptosis after *Fosl2*-knockdown, left: representative images of apoptosis

140 detected by flow cytometry, right: Proportion of Annexin-V positive cells, n=3. (G)

141 Western blot assay of apoptosis related protein contents of *Fosl2*-knockdown primary

142 GCs, left: Expression of apoptosis-related proteins, right: Mean gray values, n=3.

143 Original blots can be viewed in Figure S4A. (H) TUNEL staining of *Fosl2*-knockdown

144 cells, green represents apoptosis-positive cells, left: Representative fluorescence

145 images of TUNEL staining, right: Cell apoptosis rate. (I-L) Knockdown *Fosl2* in GCs

146 of sheep. (I) Schematic representation of the knockdown or overexpress of *Fosl2* in

147 primary GCs. (J) Efficiency analysis of *Fosl2* interference using qRT-PCR, n=3. (K)

148 Flow cytometry results of apoptosis after *Fosl2*-knockdown, left: representative images

149 of apoptosis detected by flow cytometry, right: Proportion of Annexin-V positive cells,

150 n=3. (L) TUNEL staining of *Fosl2*-knockdown cells, green represents apoptosis-

151 positive cells, left: Representative fluorescence images of TUNEL staining, right: Cell

152 apoptosis rate. Statistical significance was determined using two-tailed unpaired
153 Student's t test or chi-square test, values were mean \pm SD. Significant differences were
154 denoted by * $P < 0.05$, ** $P < 0.01$, *** $P < 0.005$, **** $P < 0.001$. The experiments were
155 repeated independently two times, yielding consistent results.

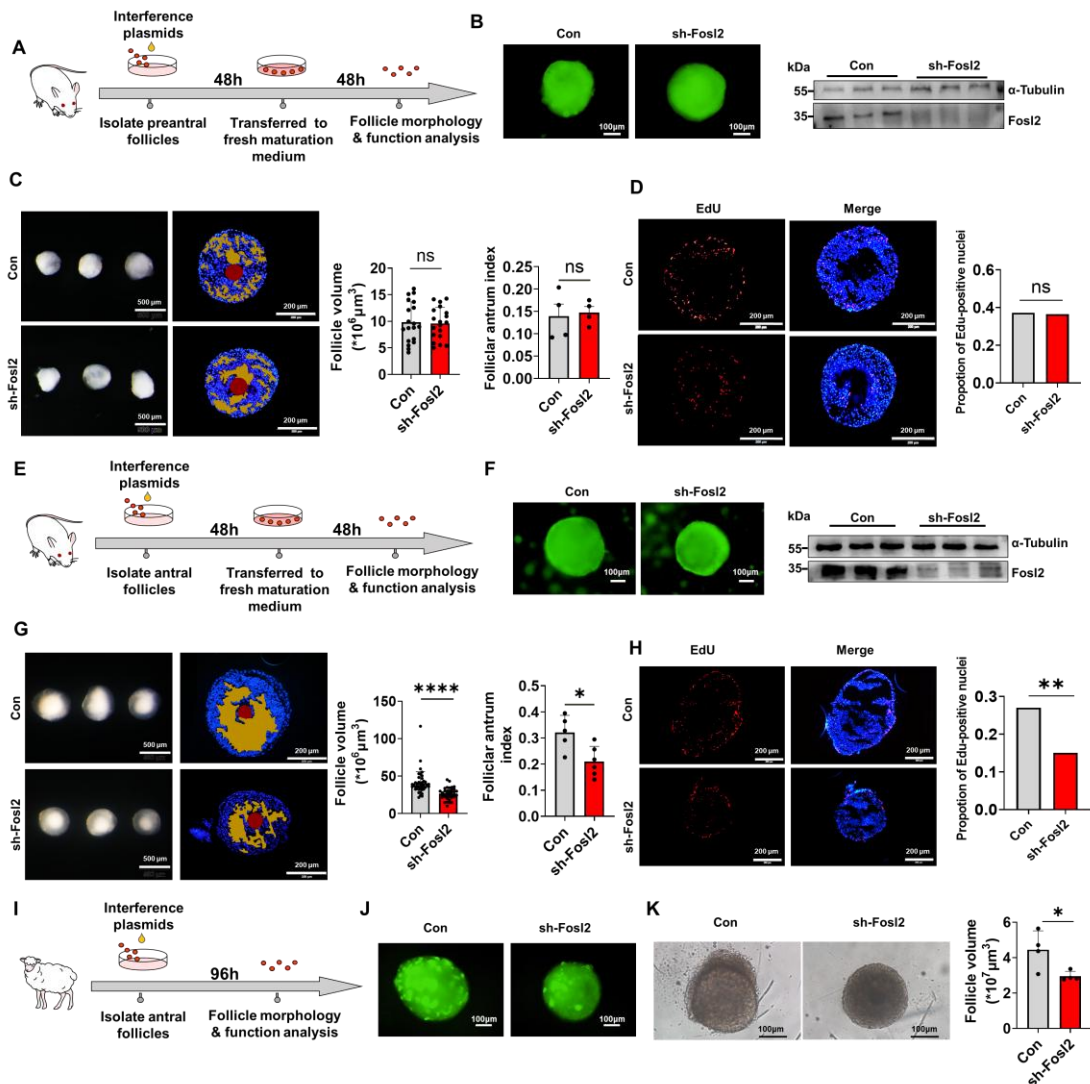
156 **3. Knockdown of *Fosl2* impairs gonadotropin-dependent folliculogenesis**

157 To investigate the direct effects of *Fosl2* on folliculogenesis, we employed a
158 previously established *in vitro* follicle culture system of mouse [33] and sheep. The
159 expression of *Fosl2* was disrupted by lentivirus transfection of shRNA in follicles at
160 different developmental stages.

161 Firstly, *Fosl2* was knocked down in the pre-antral (GTH-independent) follicles of
162 mouse (Figure 3A), and observed fluorescence at 48 h after transfection (Figure 3B).
163 After the completed transfection, the follicles were transferred to fresh maturation
164 medium and cultured for 48h. The samples were collected after the follicular cavity can
165 be clearly observed. The interference efficiency was verified by protein levels (Figure
166 3B). There was no significant difference in follicle volume and cavity area index
167 (Figure 3C). EdU staining of antral follicle sections further demonstrated no significant
168 difference (Figure 3D). Together, these data suggest that interfering with *Fosl2* in
169 secondary follicles has no significant effect on their development.

170 Subsequent investigations focused on small antral (GTH-dependent) follicles. The
171 antral follicles were transfected and collected (Figure 3E, F). Measurements revealed
172 significant reductions in follicle volume and cavity area index, indicating restraint of
173 antral cavity expansion in *Fosl2*-knockdown follicles (Figure 3G). EdU staining of
174 follicular sections demonstrated suppressed granulosa cell proliferation (Figure 3H).
175 qRT-PCR analysis further showed downregulation of proliferation-related genes
176 (*PCNA*, *Ki67*, *Cyclin E1*; Figure S2). These findings conclusively demonstrate that
177 *Fosl2*-knockdown impairs GTH-dependent folliculogenesis by suppressing antral
178 expansion and granulosa cell proliferation.

179 Moving on to sheep, *Fosl2* was knockdown in antral follicles (Fig 3I, J). Similarly,
180 the volume of *Fosl2*-knockdown follicles was significantly reduced (Fig 3K).



181

182 **Figure 3. Effect of *Fos12* knockdown on folliculogenesis at different stages.** (A-D)

183 *Fos12* was knocked down in the cultured GTH-independent follicles in vitro. (A)

184 Schematic representation of the knockdown of *Fos12* in cultured GTH-independent

185 follicles. (B) Efficiency analysis of *Fos12* interference, left: Green fluorescence

186 indicates successful transcription of interfering plasmids in follicles, right: Western blot

187 assay of protein contents of *Fos12*, n=3. Original blots can be viewed in Figure S4B.

188 The scrambled shRNA was used as *Control* in this study. (C) Changes in the GTH-

189 independent follicle volume, n=19 and follicular antrum index, n=4. (D) EdU staining

190 of GTH-independent follicles, left: Representative fluorescence images of EdU staining,

191 right: Cell proliferation rate, n=4. (E-H) *Fos12* was knocked down in the cultured GTH-

192 dependent follicles in vitro. (E) Schematic representation of the knockdown of *Fos12* in

193 cultured GTH-dependent follicles. (F) Efficiency analysis of *Fos12* interference, left:

194 Green fluorescence indicates successful transcription of interfering plasmids in follicles,

195 right: Western blot assay of protein contents of *Fos12*, n=3. Original blots can be viewed

196 in Figure S4C. (G) Changes in the GTH-dependent follicle volume, n=42 follicles

197 (Con), 37 follicles (sh-Fos12) and follicular antrum index, n=5 follicles (Con), 6

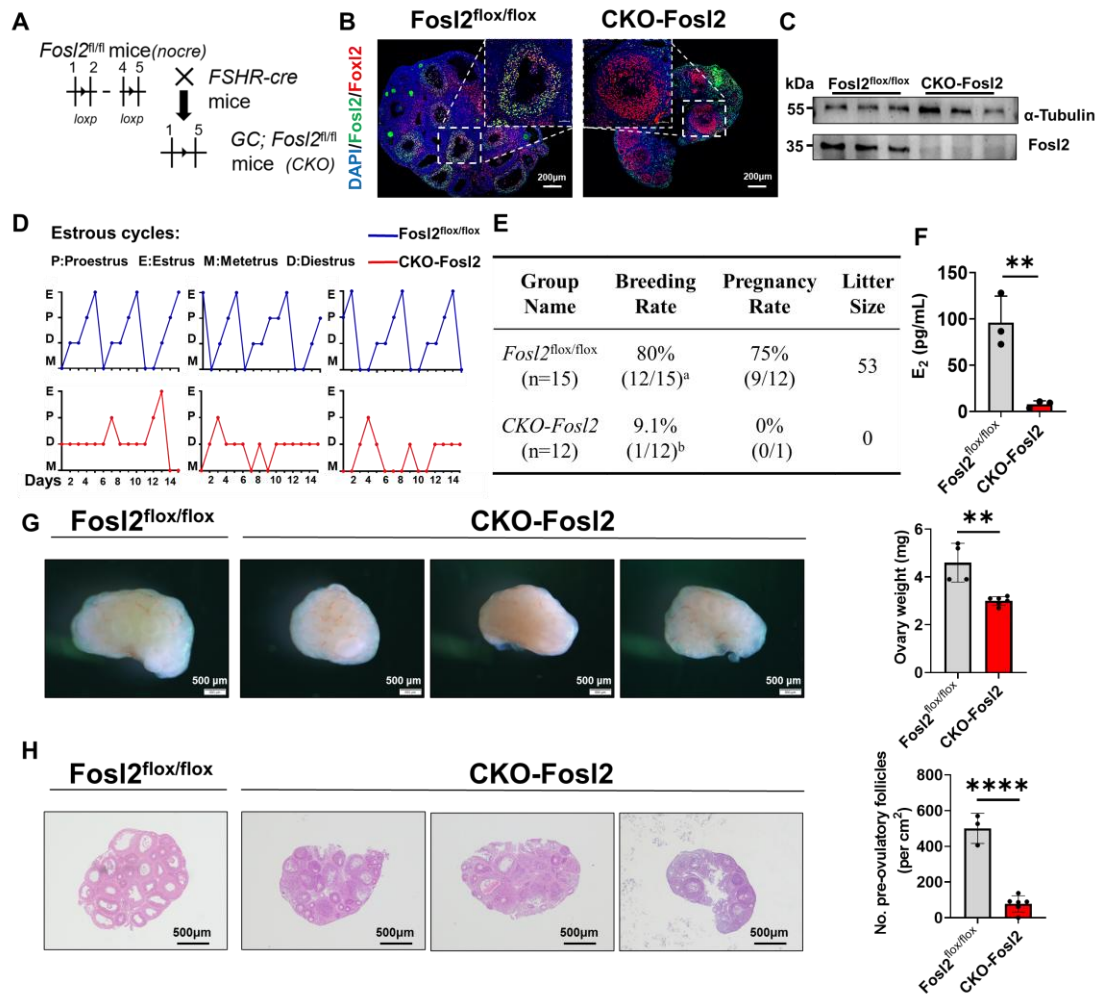
198 follicles (sh-Fos12). (H) EdU staining of GTH-dependent follicles, left: Representative

199 fluorescence images of EdU staining, right: Cell proliferation rate, n=7 follicles (Con),
200 6 follicles (sh-Fosl2). (I-K) *Fosl2* was knocked down in the cultured GTH-dependent
201 follicles of sheep in vitro. (I) Schematic representation of the knockdown of *Fosl2* in
202 cultured GTH-dependent follicles of sheep. (J) Green fluorescence indicates successful
203 transcription of interfering plasmids in follicles. (K) Changes in the GTH-dependent
204 follicle volume, n=4. Statistical significance was determined using two-tailed unpaired
205 Student's t test or chi-square test, values were mean \pm SD. Significant differences were
206 denoted by *P<0.05, **P<0.01 ****P<0.001. The experiments were repeated
207 independently two times, yielding consistent results.

208 **4. Conditional knockout of *Fosl2* in GCs leads to arrested GTH-folliculogenesis in** 209 **female mice**

210 In order to further explore the effect of *Fosl2* on GTH-dependent folliculogenesis
211 at individual level, we constructed a GCs-specific *Fosl2* knockout mouse model (*CKO*).
212 We crossed *Fosl2*^{flox/flox} with *FSHR-Cre* mice to create a *GCs-Cre; Fosl2*^{fl/fl} mouse
213 (Figure 4A). Immunofluorescence staining and WB were utilized to verify the knockout
214 efficiency (Figure 4B, C).

215 An obvious estrus cycle disorder can be observed in adult female *CKO-Fosl2* mice
216 of three estrus cycles (Figure 4D). Subsequent fertility assessments demonstrated
217 significantly reduced mating rates in *CKO* mice compared to *Fosl2*^{flox/flox} mice, with
218 only one successful mating and no pregnancy (Figure 4E), indicating *Fosl2* conditional
219 knockout induced female infertility. The serum estradiol content of mice also decreased
220 (Figure 4F). Since the estrous cycle is closely related to folliculogenesis, we counted
221 the ovarian weight of *CKO-Fosl2* mice and found that the ovarian weight decreased
222 significantly after the conditional knockout (Figure 4G), suggesting that there may be
223 abnormal folliculogenesis. HE staining of the ovarian sections at PMSG 48 h revealed
224 a significant reduction in the number of preovulatory follicles (Figure 4H), which
225 indicated that the arrested folliculogenesis led to the infertility of the mice. The
226 molecular phenotypes of ovarian GCs in *CKO* mice were also examined (Figure S3).
227 These findings collectively demonstrate that *Fosl2* knockout impedes GTH-dependent
228 folliculogenesis, ultimately leading to female infertility.



229

230 **Figure 4. *Fosl2* conditional knockout result in infertility in female mice.** (A)

231 Schematic representation of the *Fosl2* conditional knockout in GCs of mice. Exon 2-4

232 deletion via *FSHR-Cre*-mediated recombination in GCs within *GC; Fosl2^{flox/flox}*

233 (*CKO*). (B) Immunostaining showed that the *Fosl2* gene was successfully knocked

234 out in ovarian GCs of *CKO* mice, blue: DAPI, green: *Fosl2*, red: *Foxl2*. (C) Western

235 blot assay of protein contents of *CKO-Fosl2* mice, n=3. Original blots can be viewed

236 in Figure S4D. (D) Representative plot of estrous cycles, n=10. (E) Breeding rate,

237 pregnancy rates, litter size of *CKO-Fosl2* mice. (F) Effect of conditional knockout of

238 ovarian GCs on estradiol levels in serum, n=3 serum samples. (G) Morphological

239 analysis of ovary after 48 hours of PMSG treatment, left: Representative photographs,

240 right: Statistical graph, n=4 ovaries (*Fosl2^{flox/flox}*), 6 ovaries (*CKO-Fosl2*). (H) H&E

241 staining of ovaries 48 h after PMSG treatment, left: Representative photographs,

242 right: Follicle number statistics, n=3 ovaries (*Fosl2^{flox/flox}*), 6 ovaries (*CKO-Fosl2*).

243 Statistical significance was determined using two-tailed unpaired Student's t test,

244 values were mean \pm SD. Significant differences were denoted by **P<0.01

245 ****P<0.001. The experiments were repeated independently two times, yielding

246 consistent results.

247

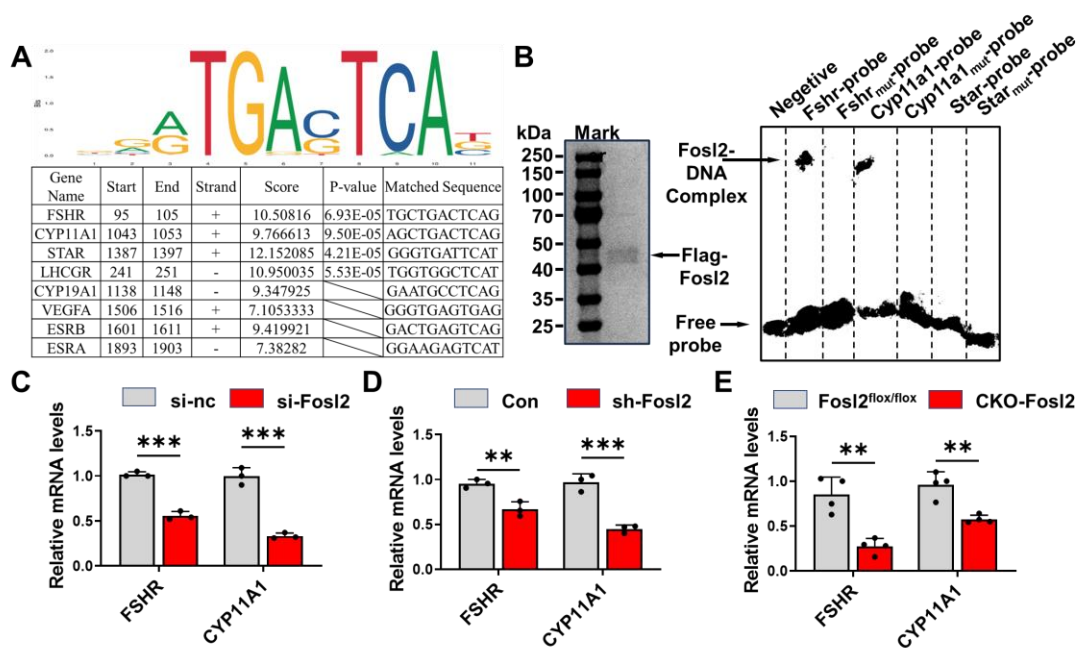
248 **5. *Fosl2* regulates FSHR and CYP11A1 transcription**

249 To elucidate the mechanism of *Fosl2* in GTH-dependent folliculogenesis, we used
250 JASPAR and FIMO databases to predict the potential binding sites of *Fosl2* protein to
251 key genes in folliculogenesis. Analysis showed that *Fosl2* may target genes that play a
252 core role in GTH-dependent folliculogenesis (Figure 5A). The EMSA result revealed
253 FOSL2 binding to the *Fshr* promoter and *Cyp11a1* promoter (Figure 5B).

254 To validate the aforementioned hypothesis, we examined the expression levels of
255 *FSHR* and *CYP11A1* in *Fosl2*-knockdown GCs using qRT-PCR. The results
256 demonstrated that *Fosl2*-knockdown significantly downregulated the mRNA
257 expression (Figure 5C). Further, qRT-PCR analysis of *Fosl2*-knockdown cultured
258 follicle model indicated the similar results (Figure 5D). Consistent results were
259 observed in GCs of *CKO* mice (Figure 5E).

260 These results suggest that FOSL2 can bind to critical genes' promoter such as *Fshr*
261 and *Cyp11a1*.

262



263

264 **Figure 5. FOSL2 directly bind to the promoter of *Fshr* and *Cyp11a1*.** (A) Prediction
 265 of possible binding sites of *Fosl2* and GTH-dependent folliculogenesis genes. (B)
 266 EMSA demonstrated FOSL2 binding to *Fshr* and *Cyp11a1* promoter sequences. (C)
 267 Expression of genes of *FSHR* and *CYP11A1* of GCs in *Fosl2*-knockdown primary GCs,
 268 n=3. (D) Expression of genes of *FSHR* and *CYP11A1* of GCs after *Fosl2* knockdown
 269 in cultured follicles, n=3. (E) Expression of genes of *FSHR* and *CYP11A1* in GCs of
 270 *CKO* mice, n=4. Statistical significance was determined using two-tailed unpaired
 271 Student's t test, values were mean \pm SD. Significant differences were denoted
 272 by * $P < 0.05$, ** $P < 0.01$, *** $P < 0.005$, **** $P < 0.001$. The experiments were repeated
 273 independently two times, yielding consistent results.

274

275 **DISCUSSION**

276 As a transcription factor affecting a variety of cells, *Fosl2* is highly expressed in
277 ovarian GCs, but its effect on folliculogenesis remains underexplored. In this study, we
278 investigated the effects of *Fosl2* on GTH-dependent follicles in vitro and in vivo. *Fosl2*
279 knockdown leads to proliferation arrest and apoptosis of primary GCs and GTH-
280 dependent follicles. Notably, we demonstrate that granulosa cell-specific *Fosl2*
281 knockout causes female infertility in mice.

282 In previous studies, *Fosl2* has been shown to be expressed and function in a variety
283 of cells and tissues. Including mediating renal tubular epithelial cell transdifferentiation
284 in fibrosis [34], suppressing myogenic differentiation in porcine muscle stem cells[35],
285 driving senescence in hepatic progenitor-like cells [36], negatively regulating NK cell
286 development [37]. The function of GCs is closely related to folliculogenesis and
287 maturation. Our identification of *Fosl2*'s ovarian enrichment and PMSG-induced
288 expression suggests its critical involvement in folliculogenesis (Figure 1). Further
289 studies showed that *Fosl2* knockout had no significant effect on the growth of GTH-
290 independent follicles, but only affected the GTH-dependent follicles (Figure 3). This
291 suggests that knockdown of *Fosl2* inhibits folliculogenesis by inhibiting granulosa cell
292 proliferation and GTH-dependent follicle antral expansion. This is also consistent with
293 the effect of *Fosl2* on inhibiting proliferation in other cells.

294 Since *Fosl2* is stably expressed during the early development of animals and total
295 deletion leads to lethality, the conditional knockout method can be adopted for the
296 research on *Fosl2* in specific tissues. Smith et al. have constructed conditional knockout
297 rats of *Fosl2* in the pineal gland [38], and Chen et al. have constructed conditional
298 knockout mice with hematopoietic system deficiency [39]. In this study, after
299 conditional knockout of *Fosl2* in mouse ovarian GCs, the mice showed disorders of
300 estrus cycles and infertility. The mating rate of CKO mice was extremely low, and they
301 did not become pregnant even after successful mating. The morphological analysis of
302 the ovaries suggested that the knockout of *Fosl2* was accompanied by a decrease in

303 preovulatory follicles, which was consistent with its inhibitory effect on the growth of
304 GTH-dependent follicles (Figure 4).

305 Bioinformatics analysis and experimental verification indicated that *Fosl2* can
306 regulate the expression of genes related to estradiol synthesis (Figure 5). This finding
307 is consistent with the conclusion that members of the AP-1 family are involved in the
308 transcription regulation of steroid synthetase [40]. At the same time, the expression of
309 genes related to granulosa cell differentiation *FSHR*, also significantly decreased while
310 the expression of genes related to estradiol synthesis *CYP11A1*, significantly decreased.
311 The direct regulation of *FSHR* and *CYP11A1* by *Fosl2* suggests that this regulation has
312 an important influence on some signaling pathways downstream of folliculogenesis [41,
313 42].

314 At present, this study still has limitations. For future studies, we will further
315 explore the signaling pathways that *Fosl2* regulate when it plays the role of regulating
316 folliculogenesis, and explore the expression and role of *Fosl2* in males. In addition, the
317 role of *Fosl2* in the regulation of folliculogenesis in sheep remains to be further studied.
318 The materials and methods employed in this study will be described in detail in the final
319 submission version.

320 In conclusion, this study demonstrates that *FOSL2* directly regulates *FSHR* and
321 *CYP11A1* transcription as an essential transcription factor for gonadotropin-dependent
322 folliculogenesis. Moreover, conditional knockout of *Fosl2* in GCs of follicles leads to
323 disrupted estrous cycles and infertility in female mice. These findings elucidate the
324 important role of *Fosl2* in the folliculogenesis process and fertility in female mice. This
325 study supplements the regulatory mechanism of GTH-dependent folliculogenesis and
326 provides a new approach for improving folliculogenesis, as well as new insights for
327 enhancing the fertility of female animals and humans.

328

329 MATERIALS AND METHODS

330 Animals

331 Kunming mice were purchased from the Center for Animal Testing of Huazhong
332 Agricultural University (Wuhan, China). *Fosl2^{fllox/fllox}* C57BL/6J mice were purchased
333 from GemPharmatech Co., Ltd., and FSHR-Cre mice were donated by Prof. Su
334 (Shandong University, China). Mice were reared in an SPF laboratory animal house, at
335 a constant temperature of $22 \pm 2^\circ\text{C}$, being allowed to access food and water ad libitum
336 with 12h light-dark cycles. Sheep samples are collected from slaughterhouses. All
337 experiments and handling of animals were approved and guided by the Institutional
338 Animal Ethics Committee of Huazhong Agricultural University Committee.

339 Construction of *Fosl2* ovarian granulosa cell conditional knockout mouse model: The
340 exon2-exon4 of the *Fosl2*-201 (ENSMUST00000031017.10) transcript was used as
341 the knockout region. Ex vivo transcription of sgRNA was carried out to construct the
342 donor vector. Cas9, sgRNA and the targeting vector were injected into the fertilized
343 eggs of C57BL/6J mice through microinjection technology. F0 generation positive
344 mice were obtained by transplantation of fertilized eggs and verified by PCR and
345 sequencing. The F0 positive mice were crossed with C57BL/6J mice to obtain stable
346 F1 generation flox heterozygous mice models. F1 generation mice were mated with
347 each other to obtain *Fosl2^{flox/fllox}* mice. *Fosl2^{flox/fllox}* mice were crossed with FSHR-Cre
348 mice to obtain the conditional knockout heterozygotic mice of *Fosl2* in granulosa cells
349 (*Fosl2^{+/-Cre}*). *Fosl2^{+/-Cre}* mice were crossed with *Fosl2^{flox/fllox}* mice to obtain the
350 conditional knockout mice of *Fosl2* in granulosa cells, *Fosl2^{flox/fllox Cre}* (CKO-*Fosl2*).

351 Superovulation

352 Mice were injected 5IU pregnant mare serum gonadotropin (PMSG) (Ningbo Sansheng
353 Biological Technology) to promote follicle growth. 48 hours after injection of PMSG,
354 5IU human chorionic gonadotropin (hCG) (Ningbo Sansheng Biological Technology)
355 was injected to promote ovulation.

356 Analysis of RNA-seq

357 The mouse transcriptome data were sequenced in-house, with granulosa cells isolated

358 from pre-ovulatory follicles at 0- and 24-hours post PMSG injection. Specific
359 transcriptome sequencing method was described in previous research [32].

360 **Analysis of qRT-PCR**

361 Total RNA from samples was extracted using TRIzol reagent (Takara, 9109, Japan) and
362 cDNA was obtained by reverse transcription using Evo M-MLV RT Kit (AGbio,
363 AG11728, China). qRT-PCR was performed by CFX384 Real-Time PCR System (Bio-
364 Rad). Reaction system includes: SYBR Green (Biosharp, China), 2 μ L complementary
365 DNA template, 250 nM of the forward and reverse primers for each, and ddH₂O was
366 supplemented to a total volume of 10 μ L. The reaction protocol was conducted as
367 described: an initial denaturation step at 95 °C for 10 min, succeeded by 35 cycles
368 comprising denaturation at 95 °C for 10 s and annealing/ extension at 60°C for 30 s.
369 Using ACTB to normalize gene expression levels, and using comparative $2^{-\Delta\Delta C_t}$
370 method to determine relative RNA quantification. The primer sequences are provided
371 in Table S1.

372 **Western Blot**

373 Extract total protein with lysis buffer consist of RIPA (ComWin Biotech, China),
374 protease and phosphatase inhibitors (ComWin Biotech, China) and PMSF (Solarbio,
375 China). Protein content was measured using BCA Protein Assay Kit (Servicebio, China).
376 Protein bands were separated sufficiently by SDS polyacrylamide gel electrophoresis
377 (SDS-PAGE) and transferred onto a polyvinylidene fluoride membrane. After blocking
378 the band with 5% skim milk powder (Nestle) at room temperature, incubated the band
379 overnight at 4°C with the primary antibodies. Primary antibodies listed as follows:
380 Fos12 (1:1000, Abclonal), α -Tubulin (1:1000, Biodragon-immunotech), Caspase3
381 (1:1000, Cell Signaling Technology), Cleaved-Caspase3 (1:1000, Abclonal), Bax
382 (1:1000, Cell Signaling Technology). Next, rinsed the bands with TBST (Servicebio,
383 China) and incubated with the secondary antibody: goat anti-rabbit immunoglobulin G
384 (1:4000, Biodragon-immunotech, China), goat anti-mouse immunoglobulin G (1:4000,
385 Biodragon-immunotech, China) for 120 min at room temperature. After rinsing with
386 TBST, the bands were visualized with ECL chemiluminescent reagent kit (Servicebio,
387 China) and acquire photographs with the Chemiluminescence Imager (Image Quant
388 LAS 4000 mini, USA). The housekeeping protein α -tubulin was used for gray value

389 statistic normalize.

390 **Immunofluorescence Staining**

391 The collected ovaries were embedded in 4% paraformaldehyde (Servicebio, China) to
392 be immobilized. After paraffin embedding, the ovaries were sliced into sections of 5
393 μm . Following dewaxing and antigen retrieval, the samples were treated with 0.5%
394 Triton-X-100 in PBS for 15 min to facilitate permeabilization, followed by blocking
395 with 5% donkey serum for 30 min. Subsequently, the sections were incubated with the
396 FOSL2 (1:100, Abclonal)/FOXL2 (1:100, Abclonal) antibody at 4°C overnight. After
397 rinsing, the sections were incubated with the goat anti-rabbit immunoglobulin G (1:
398 10000, Biodragon-immunotech, China) at 37°C for 60 min. Cell nuclei were stained
399 with DAPI at room temperature for 5 min. Next, the samples were rinsed and
400 subsequently sealed with an anti-fluorescence quencher. Images were taken using the
401 LSM800 confocal microscope system (Zeiss, Germany).

402 **Culture of primary granulosa cells**

403 Primary granulosa cells were collected after puncturing mouse or sheep ovarian
404 follicles, filtered and inoculated into culture dishes. Cells were cultured at 37 °C in a
405 5% CO₂ incubator using 10% fetal bovine serum (FBS) (Serana, Germany), DMEM/
406 F12 (Gibco, Carlsbad, CA, USA) with 1% penicillin-streptomycin (Servicebio, China).
407 Subculturing after 48 h for subsequent experiments.

408 **Culture of follicles**

409 Mouse: The follicles of different sizes were isolated from mouse ovaries using 33-gauge
410 microneedles (KONSFI, China) for the experiment of follicles at different stages. The
411 size of Small preantral follicles is 100-120 μm , and the size of antral follicles is 180-
412 200 μm . Isolated follicles were cultured in 96-well plates (BKMAM, China), covered
413 with mineral oil (Sigma, Germany), and in an incubator maintained at 37 °C and 5%
414 CO₂. The main components of follicle maturation medium include: α -MEM (Gibco,
415 USA), 5% FBS (Serana, Germany), 1% ITS (Macklin, China), 100 U/mL penicillin-
416 streptomycin (Servicebio, China) and 10 mIU/mL FSH (NSHF, China).

417 Sheep: The follicles of different sizes were isolated from sheep ovaries using
418 ophthalmic scissors and 26-gauge microneedles (KONSFI, China) for the experiment

419 of follicles at different stages. Isolated follicles were cultured in 96-well plates
420 (BKMAM, China), covered with mineral oil (Sigma, Germany), and in an incubator
421 maintained at 38.5 °C and 5% CO₂. The main components of follicle maturation
422 medium include: α-MEM (Gibco, USA), 10% FBS (Serana, Germany), 1% ITS
423 (Macklin, China), 100 U/mL penicillin–streptomycin (Servicebio, China), 50 µg/mL
424 ascorbic acid, 2 mM hypoxanthine, 2 mM glutamine and 10 mIU/mL FSH (NSHF,
425 China).

426 **RNA Interference and Overexpression**

427 Using si-RNA to inhibit the expression of target genes in Cells: When reached about
428 50% confluence, cells were transfected with siRNA using jetPRIME transfection
429 reagent. 48h later, cell samples were collected or conducted further experiments.

430 Lentivirus-mediated RNA interference was used to inhibit the expression of target
431 genes in follicles. Briefly, PLKO.1-EGFP-PURO plasmid (Genecreate, China) was
432 utilized to construct interference vectors. Small interfering RNA targeted Fosl2
433 sequence is 5'- ATCATTGACCGCTCCTTTAGGT-3'. Negative siRNA, pMD2.G and
434 pSPAX were purchased from Genecreate. Lentiviruses were produced in 293 T cells
435 (ATCC, USA) by co-transfecting 4.8 µg interference vector, 2.4 µg pMD2.G, and 3.6
436 µg pSPAX2. The viral supernatants were harvested after 48 h, centrifuged, and filtered
437 through 0.45 µm polyvinylidene fluoride membranes (Sigma, USA). Follicles with a
438 specific diameter (mouse: around 140 µm, sheep: around 300 µm) were selected for
439 GTH-independent follicle knockdown Fosl2, and follicles with a diameter of around
440 180 µm were selected for GTH-dependent follicle knockdown Fosl2 to ensure that
441 Fosl2 was knocked down before follicular antrum formation. Follicles were cultured in
442 medium with 10 µg/mL polybrene and 100 µL/mL viral supernatants (mouse: 48h,
443 sheep: 96h). The medium was replaced with normal maturation medium after the green
444 fluorescence of the follicles was observed.

445 Using plasmid to overexpression the target genes in Cells: The protein coding region of
446 mouse Fosl2 gene (CCDS: CCDS19190.1, length 981bp) was inserted into the BamHI
447 XhoI cloning site of pcDNA 3.1 plasmid to construct an overexpression vector.
448 Transfection was completed using jetPRIME transfection reagent.

449 **Flow Cytometry**

450 Cell cycle: Primary granulosa cells transfected 48 h be collected and resuspended with
451 500 μ L cold 70% ethanol at 4 $^{\circ}$ C overnight. After rinsing with PBS, the cell samples
452 were incubated with Rnase/PI at room temperature for 60 min. Early apoptosis: Primary
453 granulosa cells transfected 48 h be collected and resuspended with Annexin V-FITC
454 binding buffer. Add Annexin V-FITC/PI and incubate at RT for 15 min. Cell cycle and
455 apoptotic cells were estimated in a flow cytometer (Beckman Coulter).

456 **Real-time Cell Analysis**

457 The cellular dynamic proliferation was monitored using the RTCA DP Instrument
458 (Roche, Switzerland) based on electronic impedance detection. Cells were seeded in E-
459 plate16 at an adjusted density of 7×10^4 cells/mL. Subsequently, 100 μ L of cell
460 suspension was dispensed into each well of the E-plate16. Following a 30-minute
461 incubation at room temperature to facilitate cell sedimentation, the E-plate16 was
462 transferred to the RTCA station for continuous impedance monitoring. The proportion
463 of impedance change was continuously recorded, which was expressed by cell index,
464 with data acquisition performed at 30-minute intervals over a 160-hour observation
465 period. Cellular transfection was implemented at the 14th hour post-monitoring
466 initiation.

467 **EdU Staining**

468 Use EdU assay kit (Ribo Bio, China) to measure cell proliferation in cells and follicles.
469 Primary granulosa cells: 100 μ L 50 μ mol/L EdU be supplemented into the interfered
470 cells, and the cells were immobilized after 2h incubation. Follicles: 50 μ L 1 mg/kg EdU
471 be supplemented into the interfered follicles, after incubating 24 h, used OCT (Sakura,
472 USA) embed the follicles and frozen, and employed Cryostat (Leica, Germany) to
473 section the follicle into 5 μ m slices. Cell slides and follicle sections were incubated
474 with $1 \times$ Apollo staining solution for 30 min. The nuclei were stained with $1 \times$
475 Hoechst33342 reaction solution for 30 min. After staining and rinsing, images were
476 collected using a fluorescence microscope (Olympus, Japan).

477 **TUNEL Staining**

478 Cellular sample preparation method: The primary granulosa cell slides with interfering
479 factors were fixed with 4% paraformaldehyde (Servicebio, China) for 15 min, then

480 rinsed with PBS. Subsequently, 0.2% TritonX-100 in PBS was added and incubated at
481 37°C for 10 min. After rinsing with PBS, 100 μ L of TdT Equilibration Buffer was added
482 to each sample and incubated at 37°C for 10-30 min. The TdT Equilibration Buffer was
483 then removed and the labeling working solution was added. Incubation was carried out
484 at 37°C in the dark for 60 min. After rinsing, DAPI was added and incubated for 5 min.
485 The samples were then sealed with an anti-fluorescence quencher.
486 The preparation method for frozen sections of follicles was the same as that for EdU
487 staining. Frozen sections were fixed with 4% paraformaldehyde (Servicebio, China) for
488 30 min, rinsed with PBS, and then 5 μ g/mL proteinase K working solution was added
489 to each sample and incubated at 37°C for 10 min. The subsequent steps were the same
490 as those for cell slide staining. After staining, images were captured using a
491 fluorescence microscope (Olympus, Japan). Normal nuclei are shown in blue and
492 apoptotic cells in green. Apoptosis rate was the proportion of apoptotic cells to total cell
493 number.

494 **H&E Staining**

495 Vaginal smear staining: The dried vaginal smears were dyed with hematoxylin and
496 eosin respectively for 60 s, then fully rinsed and dried, and observed under a microscope.
497 Ovary section staining: Ovarian tissue sections were deparaffinized and rehydrated and
498 stained with hematoxylin for 6min, eosin for 20s. Then dehydrated with various
499 concentrations of alcohol and removed with xylene. Stained sections were sealed with
500 neutral gum, and images were obtained using a microscope (Olympus, Japan) for
501 analysis.

502 **Estrus cycle determination and mating**

503 Vaginal smears of sexually mature mice aged 8 weeks were collected daily for H&E
504 staining and the stage of estrus was examined for 15 days (3 estrus cycles). The mice
505 that were confirmed to be in estrus were mated with male mice at night, and the vaginal
506 plugs were checked the next morning to ensure whether the mating was successful.

507 **Prediction of binding sites**

508 JASPAR (<https://jaspar.genereg.net/>) and FIMO ([https://meme-suite.org/meme/tool](https://meme-suite.org/meme/tool-s/fimo)
509 [-s/fimo](https://meme-suite.org/meme/tool-s/fimo)) were utilized to predict the binding sites of Fosl2 protein and gonadot
510 ropin, focusing on follicle-related genes.

511 **Electrophoretic mobility shift assay (EMSA)**

512 The FOSL2 Coding sequence was cloned into the pcDNA3.1-3XFlag plasmid
513 (Addgene, China) for overexpression. Flag-tagged FOSL2 proteins were
514 immunoprecipitated using an anti-Flag antibody (Beyotime, P2271, China). The elution
515 of proteins from the antibody was carried out with elution buffer (0.1 M glycine, pH
516 2.7) and then neutralized using a neutralization buffer (1 M Tris, pH 8.5). Biotin-labeled
517 DNA probes obtained from Genecreate (China) were utilized for the DNA EMSA,
518 conducted with the Chemiluminescent EMSA Kit (Beyotime, GS009, China),
519 following the manufacturer's instructions. In brief, recombinant Flag-FOSL2 and
520 biotin-labeled DNA probes were incubated in binding buffer for 30 minutes at room
521 temperature before being separated on a 4% native polyacrylamide gel at 100 V in TBE
522 buffer (Beyotime, R0223, China). Subsequently, the DNA-protein complexes were
523 transferred onto Amersham Hybond-N⁺ membranes (Cytiva, RPN1510B, USA),
524 blotted with HRP-conjugated streptavidin, and visualized via autoradiography.

525 **Hormone Determination**

526 Estradiol in serum was detected by radioimmunoassay kit (the Bioengineering Institute
527 China). Sera were obtained by centrifuging whole blood at 3000 rpm for 10 min.
528 Detection kit was purchased from the Bioengineering Institute (Nanjing, China) and
529 commissioned the North Institute of Biological Technology (China) for testing.

530 **Statistics Analysis**

531 Statistical analyses were using GraphPad Prism 10.0 (GraphPad). Data were expressed
532 as the mean \pm SD. Two-tailed unpaired Student's t test and one-way analysis of variance
533 followed by Tukey's post hoc test were used to analyze the statistical significance
534 between two groups and among multiple groups, respectively. Chi-squared test was
535 used in the comparison between the percentages. The statistical significance was set at
536 P-value <0.05.

537

538

539 **DATA AVAILABILITY**

540 All data are available from the corresponding author upon reasonable request.

541 **FUNDING**

542 This research was supported by the Fundamental Research Funds for the Central
543 Universities (2662023DKPY001) and the National Natural Science Foundation of
544 China (31701301).

545 **SUPPORTING INFORMATION**

546 This article contains supporting information.

547 **ACKNOWLEDGEMENTS**

548 We are grateful to Prof. Yongqiang Su (Shandong University, China) and Prof. Dr.
549 Louis Dubeau (University of South California, USA) for providing the FSHR-Cre
550 mice.

551 **AUTHORS' CONTRIBUTION**

552 C.H. conceived, designed, conducted the experiments, analyzed and interpreted the data;
553 H.S., C.C. and Z.R. anticipated in experiment design and conduction, data analysis, and
554 manuscript preparation; J.L., Z.W., X.W., Y.Z., W.K., B.T. and Y.L. assisted with
555 sample collection and experiments conduction; C.H., H.S., W.R. C.C. and Z.R. wrote
556 the manuscript; X.L. and W. R. improved the manuscript. C.H., X.L., W.R. supervised
557 and funded this project. All authors approved the final version.

558 **DECLARATION OF INTERESTS**

559 The authors declare that they have no conflicts of interest with the contents of this
560 article.

561 **REFERENCES**

- 562 1. Njagi, P., et al., *Financial costs of assisted reproductive technology for patients*
563 *in low- and middle-income countries: a systematic review*. Human
564 *Reproduction Open*, 2023. **2023**(2).
- 565 2. Racowsky, C. and R.A. Satterlie, *Metabolic, fluorescent dye and electrical*
566 *coupling between hamster oocytes and cumulus cells during meiotic maturation*
567 *in vivo and in vitro*. *Dev Biol*, 1985. **108**(1): p. 191-202.
- 568 3. Sutton-McDowall, M.L., R.B. Gilchrist, and J.G. Thompson, *The pivotal role*
569 *of glucose metabolism in determining oocyte developmental competence*.
570 *Reproduction*, 2010. **139**(4): p. 685-95.
- 571 4. Pelland, A.M., H.E. Corbett, and J.M. Baltz, *Amino Acid transport mechanisms*
572 *in mouse oocytes during growth and meiotic maturation*. *Biol Reprod*, 2009.
573 **81**(6): p. 1041-54.
- 574 5. Chen, Y., S. Wang, and C. Zhang, *The Differentiation Fate of Granulosa Cells*
575 *and the Regulatory Mechanism in Ovary*. *Reprod Sci*, 2024.
- 576 6. Richards, J.S. and S.A. Pangas, *The ovary: basic biology and clinical*
577 *implications*. *J Clin Invest*, 2010. **120**(4): p. 963-72.
- 578 7. Liu, W., et al., *Transcriptome Dynamics and Cell Dialogs Between Oocytes and*
579 *Granulosa Cells in Mouse Follicle Development*. *Genomics Proteomics*
580 *Bioinformatics*, 2024. **22**(2).
- 581 8. Bosdou, J.K., et al., *Association of Basal Serum Androgen Concentration with*
582 *Follicles Number on the Day of Triggering Final Oocyte Maturation in Low*
583 *Responders According to the Bologna Criteria: A Prospective Cohort Study*. *Int*
584 *J Mol Sci*, 2025. **26**(4).
- 585 9. Wang, X., et al., *Granulosa Cell-Layer Stiffening Prevents Escape of Mural*
586 *Granulosa Cells from the Post-Ovulatory Follicle*. *Adv Sci (Weinh)*, 2024.
587 **11**(33): p. e2403640.
- 588 10. Knox, R.V., *Follicle development in pigs: State of the art*. *Mol Reprod Dev*,
589 2023. **90**(7): p. 480-490.
- 590 11. Nilsson, E.E., C. Detzel, and M.K. Skinner, *Platelet-derived growth factor*
591 *modulates the primordial to primary follicle transition*. *Reproduction*, 2006.
592 **131**(6): p. 1007-15.
- 593 12. Liu, X.M., et al., *Mitochondrial Function Regulated by Mitoguardin-1/2 Is*
594 *Crucial for Ovarian Endocrine Functions and Ovulation*. *Endocrinology*, 2017.
595 **158**(11): p. 3988-3999.
- 596 13. Knight, P.G., L. Satchell, and C. Glister, *Intra-ovarian roles of activins and*
597 *inhibins*. *Mol Cell Endocrinol*, 2012. **359**(1-2): p. 53-65.
- 598 14. Nishigaki, A., et al., *HIF-1 α Promotes Luteinization via NDRG1 Induction in*
599 *the Human Ovary*. *Biomedicines*, 2025. **13**(2).
- 600 15. Knapp, E.M., et al., *Nuclear receptor Ftz-f1 promotes follicle maturation and*
601 *ovulation partly via bHLH/PAS transcription factor Sim*. *Elife*, 2020. **9**.
- 602 16. Castrillon, D.H., et al., *Suppression of ovarian follicle activation in mice by the*
603 *transcription factor Foxo3a*. *Science*, 2003. **301**(5630): p. 215-8.

- 604 17. Renoux, F., et al., *The AP1 Transcription Factor Fosl2 Promotes Systemic*
605 *Autoimmunity and Inflammation by Repressing Treg Development*. Cell Rep,
606 2020. **31**(13): p. 107826.
- 607 18. Li, S., et al., *Fos-like antigen 2 (FOSL2) promotes metastasis in colon cancer*.
608 Exp Cell Res, 2018. **373**(1-2): p. 57-61.
- 609 19. Wu, L., et al., *Natural Coevolution of Tumor and Immunoenvironment in*
610 *Glioblastoma*. Cancer Discov, 2022. **12**(12): p. 2820-2837.
- 611 20. Zheng, S. and Y. Liu, *Progress in the Study of Fra-2 in Respiratory Diseases*.
612 Int J Mol Sci, 2024. **25**(13).
- 613 21. Chen, D., et al., *TXNDC9 promotes hepatocellular carcinoma progression by*
614 *positive regulation of MYC-mediated transcriptional network*. Cell Death Dis,
615 2018. **9**(11): p. 1110.
- 616 22. Stellato, M., et al., *The AP-1 transcription factor Fosl-2 drives cardiac fibrosis*
617 *and arrhythmias under immunofibrotic conditions*. Commun Biol, 2023. **6**(1):
618 p. 161.
- 619 23. Rampioni Vinciguerra, G.L., et al., *Role of Fra-2 in cancer*. Cell Death Differ,
620 2024. **31**(2): p. 136-149.
- 621 24. He, J., et al., *miR-597 inhibits breast cancer cell proliferation, migration and*
622 *invasion through FOSL2*. Oncol Rep, 2017. **37**(5): p. 2672-2678.
- 623 25. Sun, X., et al., *miR-143-3p inhibits the proliferation, migration and invasion in*
624 *osteosarcoma by targeting FOSL2*. Sci Rep, 2018. **8**(1): p. 606.
- 625 26. Hu, Y., et al., *LncRNA GSTM3TV2 Promotes Cell Proliferation and Invasion*
626 *via miR-597/FOSL2 Axis in Hepatocellular Carcinoma*. Biomed Res Int, 2021.
627 **2021**: p. 3445970.
- 628 27. Eferl, R., et al., *Development of pulmonary fibrosis through a pathway involving*
629 *the transcription factor Fra-2/AP-1*. Proc Natl Acad Sci U S A, 2008. **105**(30):
630 p. 10525-30.
- 631 28. Birnhuber, A., et al., *Transcription factor Fra-2 and its emerging role in matrix*
632 *deposition, proliferation and inflammation in chronic lung diseases*. Cell Signal,
633 2019. **64**: p. 109408.
- 634 29. Ucero, A.C., et al., *Fra-2-expressing macrophages promote lung fibrosis in*
635 *mice*. J Clin Invest, 2019. **129**(8): p. 3293-3309.
- 636 30. Zou, L., et al., *Bioinformatics analysis of the common targets of miR-223-3p,*
637 *miR-122-5p, and miR-93-5p in polycystic ovarian syndrome*. Front Genet, 2023.
638 **14**: p. 1097706.
- 639 31. Southall, J., et al., *Granulosa cell expression of Fos is critical for regulating*
640 *ovulatory gene expressions in the mouse ovary*. Faseb j, 2025. **39**(4): p. e70388.
- 641 32. Chen, Y., et al., *A mouse model reveals the events and underlying regulatory*
642 *signals during the gonadotrophin-dependent phase of follicle development*.
643 Molecular Human Reproduction, 2020. **26**(12): p. 920-937.
- 644 33. Wang, X., et al., *The FSH-mTOR-CNP signaling axis initiates follicular antrum*
645 *formation by regulating tight junction, ion pumps, and aquaporins*. J Biol Chem,
646 2023. **299**(8): p. 105015.

- 647 34. Liu, N., et al., *FOSL2 participates in renal fibrosis via SGK1-mediated*
648 *epithelial-mesenchymal transition of proximal tubular epithelial cells*. J Transl
649 Int Med, 2023. **11**(3): p. 294-308.
- 650 35. Zhou, P., et al., *Identification of novel transcription factors regulated by H3K27*
651 *acetylation in myogenic differentiation of porcine skeletal muscle satellite cells*.
652 Faseb j, 2024. **38**(21): p. e70144.
- 653 36. Ding, M., et al., *Integration of ATAC-Seq and RNA-Seq reveals FOSL2 drives*
654 *human liver progenitor-like cell aging by regulating inflammatory factors*.
655 BMC Genomics, 2023. **24**(1): p. 260.
- 656 37. Schnoegl, D., et al., *Fra-2 Is a Dominant Negative Regulator of Natural Killer*
657 *Cell Development*. Front Immunol, 2022. **13**: p. 909270.
- 658 38. Smith, M., et al., *Tissue-specific transgenic knockdown of Fos-related antigen*
659 *2 (Fra-2) expression mediated by dominant negative Fra-2*. Mol Cell Biol, 2001.
660 **21**(11): p. 3704-13.
- 661 39. Chen, J., et al., *Fosl2 Deficiency Predisposes Mice to Osteopetrosis, Leading to*
662 *Bone Marrow Failure*. The Journal of Immunology, 2024. **212**(7): p. 1081-1093.
- 663 40. Nguyen, H.T., M. Najih, and L.J. Martin, *The AP-1 family of transcription*
664 *factors are important regulators of gene expression within Leydig cells*.
665 Endocrine, 2021. **74**(3): p. 498-507.
- 666 41. Cai, J., et al., *Poor ovarian response to gonadotropin stimulation is associated*
667 *with low expression of follicle-stimulating hormone receptor in granulosa cells*.
668 Fertil Steril, 2007. **87**(6): p. 1350-6.
- 669 42. Li, Y., et al., *LHCGR and ALMS1 defects likely cooperate in the development*
670 *of polycystic ovary syndrome indicated by double-mutant mice*. Journal of
671 Genetics and Genomics, 2021. **48**(5): p. 384-395.
- 672